Sofosbuvir inhibits the RNA dependent RNA polymerase activity of non-Structural protein 5 from Kyasanur forest disease virus

Mansi Malik, Parvathy Vijayan, Deepak K Jagannath, Rakesh K Mishra, Anirudha Lakshminarasimhan*

Correspondence

Tata Institute for Genetics and Society, Centre at inStem, NCBS campus, GKVK, Bellary Road, Bengaluru - 560065, KA, India

Email: anirudha.l@tigs.res.in

Abstract

Kyasanur forest disease is a neglected zoonotic disease caused by a single stranded RNA based flavivirus, the incidence of which, was first recorded in 1957, in the Southern part of India. Kyasanur forest disease virus is transmitted to monkeys and humans, through the infected tick bite of *Haemophysalis spinigera*. Kyasanur forest disease is a febrile illness, which in severe cases, results in neurological manifestations leading to mortality. The current treatment regimens are symptomatic and supportive in nature. There are no targeted therapies available for this disease. In this study, we evaluated the ability of the FDA approved drug, Sofosbuvir to inhibit the RNA dependent RNA polymerase activity of NS5 protein from Kyasanur forest disease virus. NS5 protein containing the N-terminal methyl transferase domain and C-terminal RNA dependent RNA polymerase domain was expressed in *Escherichia coli* and RNA dependent RNA polymerase activity, demonstrated with the purified protein. The RNA dependent RNA polymerase assay conditions were optimized, followed by determination of apparent $K_{m,ATP}$. IC_{50} of Sofosbuvir against RNA

dependent RNA polymerase activity was determined under the optimized conditions with the purified NS5 protein. Drug repurposing strategies can accelerate the development of targeted therapies for Kyasanur forest disease. This is the first demonstration of inhibition of RNA dependent RNA polymerase activity of Kyasanur forest disease virus with a small molecule inhibitor.

Introduction

Kyasanur forest disease (KFD) is an infectious viral haemorrhagic disease primarily infecting Human and non-Human primates (1). Mortality in monkeys, especially among the black-faced langurs (*Presbytis entellus*) and red-faced bonnet monkeys (*Macaca radiata*) has been reported during multiple outbreaks of this disease (2). In addition, birds, squirrels, gerbils, mice, rats, and bats also function as hosts for the virus (3). The hard bodied tick, *Haemaphysalis spinigera*, was identified as the primary vector for Kyasanur forest disease virus (KFDV) (4). KFDV has also been isolated from various genera of ticks such as *Ixodes, Argas, Ornithodoros, Hyalomma, Dermacentor and Rhipicephalus* (3). Clinical symptoms of KFD include high grade fever, chills, intense frontal headache, sore-throat, vomiting, diarrhoea, severe myalgia, muscle tenderness, photophobia, nausea, and persistent cough (5,6). In severe cases, neurological and haemorrhagic manifestations are observed (7), with a mortality of ~ 2-10% (5,7). ICMR-NIV and Molbio Diagnostics, Goa, have developed a microchip-based point-of-care test (Truenat KFD), which is currently the gold standard for diagnosis in India (8,9). Formalin inactivated tissue-culture vaccine is available for KFD, which is administered in two doses to individuals aged 7–65 years, at one month

interval (10). However, the immunity conferred by this vaccine is short-lived, because of which booster doses are recommended after 6-9 months of primary vaccination, for five consecutive years (10). Current treatment regimens for KFD are limited to providing symptomatic relief and management (11). There are no direct acting antiviral drugs available against KFD. Failure of optimal coverage provided by the vaccine, with the absence of anti-viral interventions against KFDV, makes it a public health challenge, necessitating attention towards the development of second-generation vaccines and targeted therapies.

KFDV is a spherical (~40-65 nm in size) virus, containing an icosahedral nucleocapsid enclosing a positive-sense RNA of 10,774 bases (12). Kyasanur forest disease virus genome is closely related to Omsk hemorrhagic fever virus from Siberia, Alkhurma Virus from Saudi Arabia and Nanjianyin Virus from China (13-15). The RNA strand codes for a polyprotein comprising of three structural (C, E & M) and seven non-structural proteins (NS1, NS2a, 2b, NS3, NS4a, 4b, and NS5 (6,16). NS5 is a bi-functional protein, comprising of an N-terminal methyl transferase domain (MTase) and a C-terminal RNA-dependent RNA polymerase domain (RdRp) separated by a linker (17, 18)(Fig. 1A). MTase domain methylates N-7 of guanine and 2’-OH ribose of viral RNA cap, in the presence of S-adenosyl methionine as a co-factor. N-7 methylation is critical for the enhancement of the efficiency of viral translation, and 2′-O methylation is important for subversion of innate immune response during viral infection (18). RdRp domain of flaviviruses catalyse the de novo template-dependent formation of phosphodiester bonds in the presence of nucleoside triphosphate (NTP) and divalent metal ions. The canonical structure of flaviviridae RdRp

domain consists of an encircled right hand containing three subdomains - thumb, palm and fingers folded, surrounding the active site. RdRps consist of channels, the entry of which is lined with positively charged residues, facilitating the entry of NTPs and template RNA into the active site (17). Absence of proof-reading exonuclease activity in RdRps may lead to the incorporation of mutations, and consequently, selection of variants of viruses (19). Hence, RdRp of NS5 plays a crucial role in viral genome replication and therefore, can serve as a potential anti-viral drug target (20). In fact, nucleoside and non-nucleoside inhibitors against NS5 RdRp from different viruses belonging to the flaviviridae family has been identified (21-28).

In this study, we recombinantly expressed KFDV NS5 protein and characterized the purified protein with the objective of identifying a potential inhibitor of RdRp activity. We selected FDA approved drugs, Sofosbuvir and Dasabuvir, currently in use for the treatment of Hepatitis C virus (HCV) infection (29, 30) and evaluated their ability to inhibit the RdRp activity of KFDV NS5 protein.

Methods

Expression and purification of NS5 from KFDV

Codon optimized gene corresponding to 5 to 897 amino acids of KFDV NS5 with an N-terminal Hexa-histidine tag was synthesized (Genscript USA) and sub-cloned into pET-28a(+) vector between NdeI and HindIII restriction sites. Transformants of Rosetta2(DE3) pLysS containing pET28a – KFDV NS5 was grown to an OD of 2.0 and induced with 0.5 mM IPTG for 16 hours at 18°C. Induced cells were centrifuged at 5000 g for 10 minutes at 4°C and the pellet, resuspended in a lysis Buffer containing 20 mM Na_2HPO_4, 0.5 M NaCl, 50 mM L-Arginine, 10 mM $MgSO_4$, 5

mM β-mercaptoethanol, 5 mM Imidazole, 1 mM PMSF, 10% Glycerol, pH 7 (31). The cell suspension was sonicated, and lysate centrifuged at 20000 g for 60 minutes at 4°C. The clarified lysate was filtered with Durapore PVDF 0.22 µm membrane and loaded onto a Ni-NTA affinity column pre-equilibrated with 20 mM Na_2HPO_4, 0.5 M NaCl, 10 % Glycerol pH 7.0. The column was washed with equilibration buffer containing 50 mM Imidazole and bound protein eluted with 20 mM Na_2HPO_4, 0.5 M NaCl, 400 mM Imidazole, 10% Glycerol pH 7.0. Eluates containing a prominent band corresponding to the expected molecular weight of ~104 kDa was injected into Superdex 200 Increase 10/300 GL column pre-equilibrated with 50 mM Tris-HCl pH 8.0, 150 mM NaCl, 5 mM $MgCl_2$, 1 mM DTT, 5% Glycerol, 0.05% Tween 20. The purified protein was quantified using Bradford assay and densitometry analysis. Purified fractions were transferred onto PVDF membrane and probed with mouse anti-His primary antibody (1:3000) and anti-mouse IgG HRP—conjugate (1:6000). Gel peptic digest and LC-MS/MS analysis was performed for the gel filtration fractions to ascertain the identity of NS5 protein.

Differential scanning fluorimetry

Differential scanning fluorimetry (DSF) was performed with 5 µM NS5 protein in a buffer containing 50 mM Tris pH 7.5, 100 mM KCl, 10% glycerol, 0.1 mM MnCl2, 0.1 mM MgCl2, in triplicates using Nanotemper 6 Tycho (NanoTemper® Technologies GmbH) with a temperature gradient of 35°C to 95°C using a 30°C/min temperature ramp. Intrinsic fluorescence was detected at wavelengths of 330 nm and 350 nm, and the ratio plotted as a function of temperature. Inflection temperature, the temperature at which half of the protein species is unfolded, was determined from the melt curves (32).

RNA dependent RNA polymerase activity of purified NS5

RNA dependent RNA polymerase (RdRp) activity of KFDV NS5 protein was determined by employing an endpoint fluorometric assay based on the intercalating property of a fluorescent dye, SYTO 9, which binds to double stranded (ds) RNA and not to single stranded (ss) RNA (33). 250 nM of purified NS5 protein was added to a standard reaction mix comprising of 50 mM HEPES pH 7.0, 2.5 mM $MnCl_2$, 500 µM ATP, 20 µg/mL poly(U) and 0.1 mg/mL BSA and the reaction mix was incubated at 30°C for 60 minutes in a 96 well flat-bottom black plates. The reaction was quenched by adding 25 mM EDTA, following which 0.25 µM SYTO 9 was added and further incubated at room temperature for 7 minutes. Fluorescence was recorded in a plate reader (Infinite 200 Pro M Plex, TECAN, Switzerland) using excitation and emission filters at 485 nm and 520 nm, respectively. The background fluorescence levels were subtracted from the samples using a protein blank control reaction. The effect of pH, temperature, NaCl, and glycerol concentrations on RdRp activity was determined to identify the optimal conditions using the purified KFDV NS5 protein (34). Buffers with pH ranging from 5.0 to 9.0 (Citrate pH 5.0, Tricine pH 6.0, HEPES pH 7.0, Tris-HCl PH 7.5, Tris-HCl pH 8.0, and Bicine pH 9.0) were assayed. NS5 protein was incubated at different temperatures of 20°C, 25°C, 30°C, 37°C, and 42°C, different NaCl concentrations (5 mM, 25 mM, 50 mM, 75 mM, 100 mM, 300 mM and 500 mM) and varying percentages of glycerol (5% v/v, 10% v/v, 20% v/v, 30% v/v, 40% v/v, 50% v/v). The mean values were computed from the experiments with standard deviation.

Determination of apparent $K_{m,ATP}$

NS5 protein was titrated against a fixed concentration of 500 µM ATP, to arrive at the protein concentration of 250 nM for the determination of apparent $K_{m,ATP}$. ATP, at concentrations ranging from 50 µM to 500 µM was titrated with 250 nM of purified NS5 protein and 20 µg/mL of poly(U). Mean values were computed with standard deviations (n = 3) and K_m calculated using GraphPad Prism, 9.3.0.

Determination of inhibitory concentrations for sofosbuvir and dasabuvir

Sofosbuvir and Dasabuvir (MedChemExpress, Monmouth Junction, NJ) were dissolved in DMSO and diluted freshly for the experiment. The inhibitory effect of Sofosbuvir and Dasabuvir were determined at different concentrations ranging from 5 µM to 20 µM. The assay was performed in presence of 250 nM of NS5 protein, 20 µg/mL poly(U) and 500 µM ATP in the reaction buffer containing 50 mM HEPES pH 7.0, 5 mM NaCl, 10% glycerol, 0.1 mg/ml BSA. IC_{50} values were determined using non-linear regression model with GraphPad Prism, 9.3.0. The mean values were computed with standard deviation (n = 3).

Results

KFDV NS5 was expressed in bacteria and purified with affinity column and size exclusion chromatography

Multiple sequence alignment of KFDV polyprotein (Uniprot id: D7RF80) with NS5 proteins from tick borne encephalitis virus (TBEV), Yellow fever virus (YEFV), Zika virus (ZKV), Japanese encephalitis virus (JAEV), West Nile virus (WNV) and Dengue virus serotype 2 (DENV2), led to the identification of KFDV NS5 protein i.e., between amino acids, 2514 to 3416 in the polyprotein sequence. NS5 protein is widely

conserved across the flaviviridae family (50 – 70% identity/similarity). Residues 5 to 897 of NS5 protein containing the MTase and RdRp domain (Fig. 1A) was expressed with an N-terminal hexa-histidine tag in bacteria and purified with Ni-NTA affinity chromatography (Fig. 1B). A lower molecular weight contaminant band (Fig. 1) was observed along with the band corresponding to the expected molecular weight of NS5 (~104 kDa), on the Coomassie blue stained SDS-PAGE gel. Anti-His antibody also recognized the lower molecular weight contaminant band with western blotting, suggesting it to be an N-terminal degradation product, which was confirmed with amino acid sequencing of tryptic digests with LC-MS/MS. The sequence corresponded to 5 to 282 amino acids of the NS5 protein (Data not shown). This histidine tagged N-terminal fragment co-eluting with NS5 protein in affinity chromatography was removed with superdex 200 increase 10/300 GL size exclusion column chromatography (Peak P2 from Fig. 1C), to the extent that it was not observed in a Coomassie stained SDS-PAGE gel. The identity of the NS5 protein - Peak, P1 corresponding to the expected molecular weight of 104 kDa, was confirmed with amino acid sequencing utilizing LC-MS/MS and anti-His antibody (Fig. 1D). The yield of NS5 protein after size exclusion chromatography (P1 fraction) was 1 mg/litre of bacterial culture.

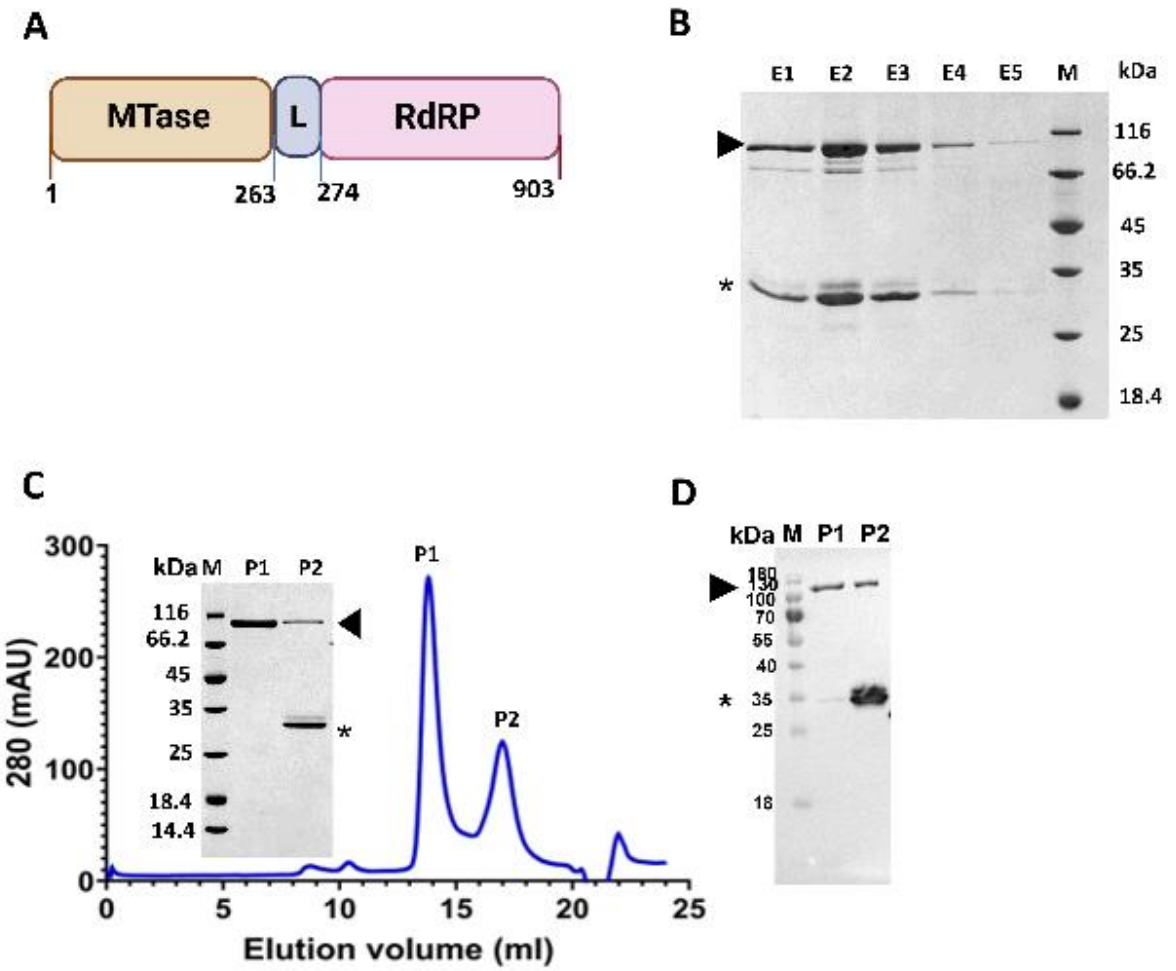

Fig. 1. NS5 protein of Kyasanur forest disease virus. A. Schematic representation of NS5 protein domains - N-terminal methyl transferase (MTase – 1 to 263) and C-terminal RNA dependent RNA polymerase (RdRp – 274 to 903). Linker (L – 264 to 273 amino acids) residues connecting the two domains are not conserved among flaviviruses (35). B. Coomassie stained SDS-PAGE gel (12%) containing Ni-NTA affinity column elutes. Lanes containing a prominent band of the expected molecular weight of 104 kDa, corresponding to 5 to 897 amino acids of NS5 are seen in the elutes (indicated by an arrow). Also seen is a lower molecular weight band, between the molecular weight markers – 35 kDa and 25 kDa (*). C. Superdex increase 200 10/300 GL fractionation of affinity purified fraction of NS5 protein. Peaks P1 and P2 correspond

to NS5 and the lower molecular weight protein (*). Coomassie stained SDS-PAGE gel is on the left panel. D. anti- Histidine tagged antibody probed western blot of P1 and P2 fractions. The prominent bands in P1 (NS5 protein indicated with arrowhead) and P2 (lower molecular weight contaminant band indicated with asterisks) was recognized by anti-His antibody.

Differential scanning fluorimetry

The thermal stability of buffer exchanged NS5 protein was determined with an intrinsic fluorescence-based differential scanning fluorimetry (DSF), in which the unfolding of protein was monitored with increasing temperature (Fig. 2). The melting temperature was determined to be 50 ± 0.2°C (n=3). As compared to the previous report employing sypro orange-based method with the full length NS5 protein from DENV4 (36), the melting temperature of KFDV NS5 was higher by ~ 12.5 °C. This could be because of the differences in amino acid composition between the viruses and/or a difference in the method employed to determine the melting temperature.

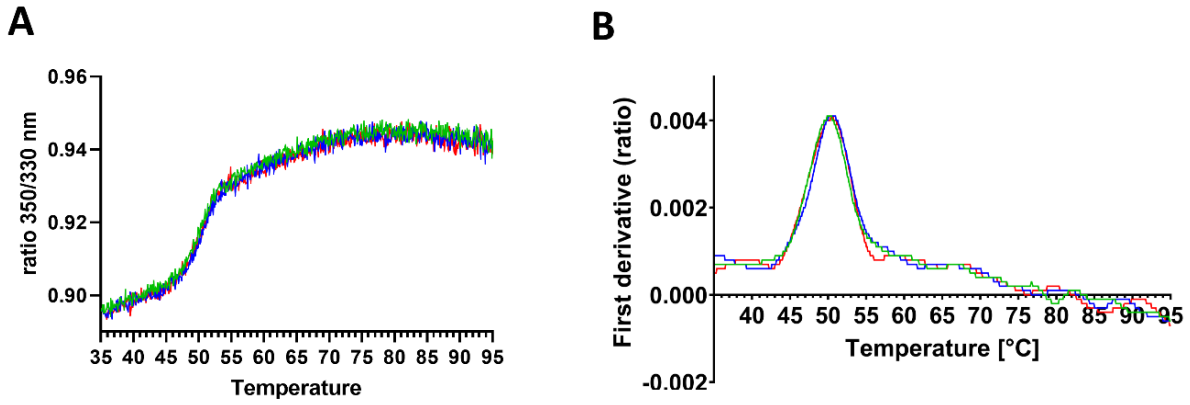

Fig. 2. Differential scanning fluorimetry profile with purified NS5 protein. A. Ratio of fluorescence emission between 350 nm and 330 nm as a function of increase in temperature, using a thermal ramp in

Tycho NT6. B. First derivative (ratio) as a function of temperature. Each experiment was performed in triplicates and repeated thrice. The graph is a representative of one experiment, in which the triplicates are shown in different colours.

Assay conditions were optimized for RNA dependent RNA polymerase activity of KFDV NS5

KFDV NS5 construct containing both the MTase and RdRp domains was used in this study, to rule out any effect of MTase domain on RdRp activity. Interplay of both RdRp and MT domain was earlier demonstrated for Zika NS5 (37). In comparison to 5% glycerol, KFDV NS5 showed an increase in RdRp activity at 10% glycerol, which significantly reduced at 20% glycerol. Low concentrations of NaCl inhibited RdRp activity of KFDV NS5, consistent with an earlier report from Usutu virus NS5 (34). RdRp from Hepatitis C Virus tolerated NaCl concentrations until 100 mM without any significant loss of RdRp activity (38). However, it is not clear as to how Dengue and KFDV/Usutu NS5 proteins differ in their sensitivity to different concentrations of NaCl. Mechanistically, binding of Dengue NS5 to ssRNA has been shown to release six Na+ ions (39). Based on this report, the loss of activity can be speculated to be due to dissociation of RNA, at higher concentrations of NaCl, and not due to denaturation of protein. At a pH of 7.0, maximal activity was observed, which tapered at pHs of 5.0 and 9.0. Optimal activity was observed at a temperature of 30°C at pH 7, without significant loss of activity at 42°C (Fig. 3) (T_m was determined to be 50°C with DSF).

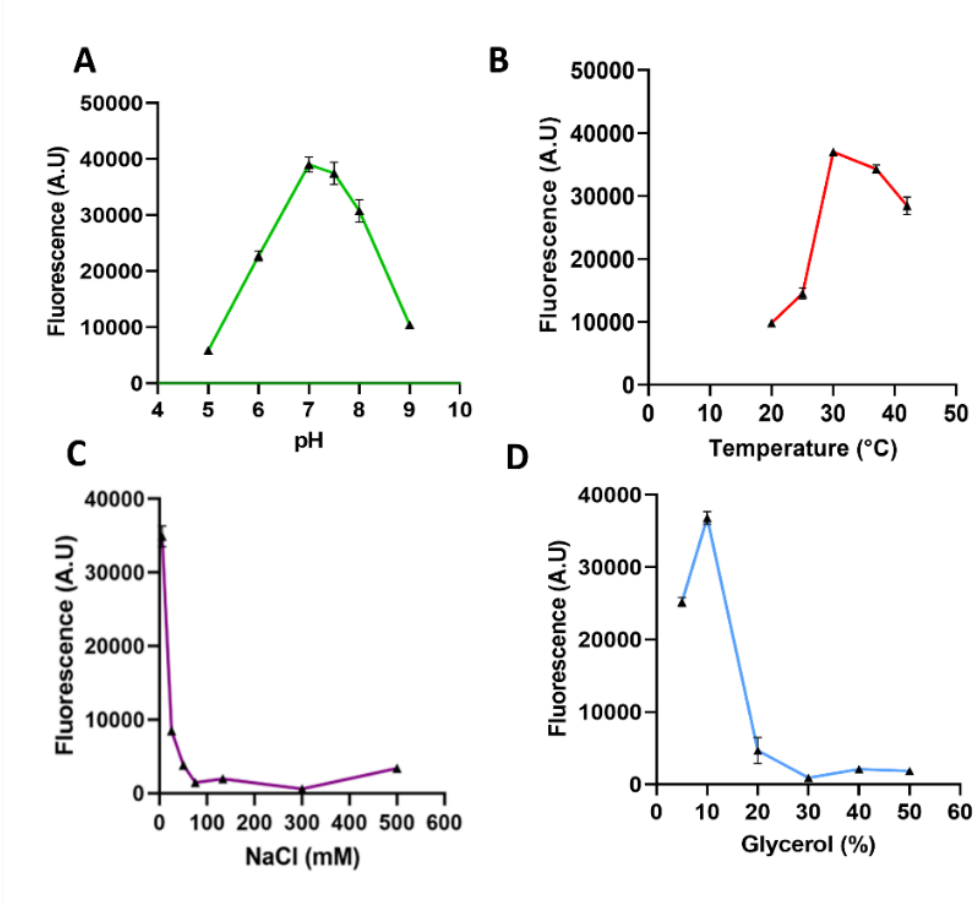

Fig. 3. Optimization of reaction conditions for RdRp activity of KFDV NS5. Effect of pH (A), NaCl (B), glycerol (C) and temperature (D) on RdRp activity. For every sample well, fluorescence units were subtracted from a blank control, devoid of NS5 protein under the same set of conditions. The standard deviation was computed, represented as error bars for every data point. Activity is represented as arbitrary fluorescence units (A.U.) in the Y-axis.

Apparent $K_{m,ATP}$ of NS5 RDRP

Apparent $K_{m,ATP}$ was determined to be 68.26 ± 0.90 µM for KFDV NS5, under the tested conditions, as described in methods (Fig. 4). The reported values of $k_{m,GTP}$ for glutathionylated Dengue and Zika NS5 were 189.8 ± 52.5 µM, and 137.2 ± 41.3 µM, respectively (39). Motif F from the ring domain of RdRp with highly conserved Lys, Glu, Arg residues, and motif

G from pinky finger domain, with conserved ala, binds to NTPs, and +1/+2 junction of template strand, respectively (Fig. 5)(40, 41). The comparable value of apparent $K_{m,ATP}$ validated the use of the purified protein for inhibition studies.

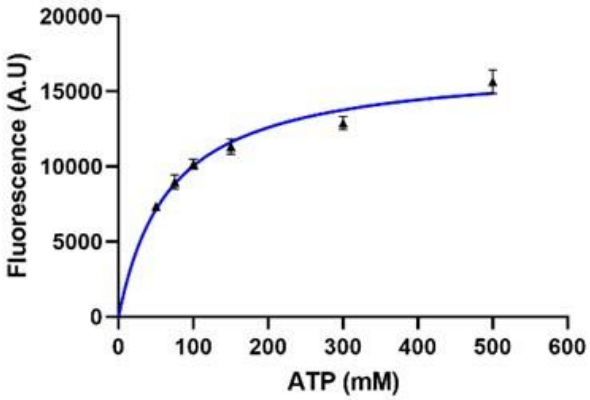

Fig. 4. Determination of apparent $K_{m,ATP}$ for RdRp domain of KFDV NS5. K_m for ATP were determined by Michaelis-Menten (Hill slope = 1) and using graph pad prism 9.3.0. The representative graph contains values averaged from at least three independent experiments. The standard deviation error bars are shown for every data point. Activity is represented as arbitrary fluorescence units (A.U.) in the Y-axis.

Sofosbuvir inhibits the RDRP activity of KFDV NS5

IC_{50} s with sofosbuvir triphosphate and sofosbuvir with HCV NS5 were determined to be 0.12 µM and 3.89 µM, respectively (27, 41). X-ray crystal structure of HCV NS5B with sofosbuvir (PDB: 4WTG), showed a critical interaction of Asn291 with 2'-F group of Sofosbuvir, leading to its incorporation into the growing RNA chain and subsequently, chain termination (Fig. 5) (42).

```
                                  Motif F
KFDV        452 VYNMMGKREKKLG----------EFGVAKGSRAIWYM 478
ALKV        452 VYNMMGKREKKLG----------EFGVAKGSRAIWYM 478
TBEV        452 VYNMMGKREKKLG----------EFGVAKGSRAIWYM 478
YEFV        452 EYNMMGKREKKLS----------EFGKAKGSRAIWYM 478
ZKV         452 VYNMMGKREKKQG----------EFGKAKGSRAIWYM 478
JAEV        453 IYNMMGKREKKPG----------EFGKAKGSRAIWFM 479
WNV         453 IYNMMGKREKKPG----------EFGKAKGSRAIWFM 479
DEN_V2      450 VYNMMGKREKKLG----------EFGKAKGSRAIWYM 476
HCV         129 DTTIMAKSEVFCVQPEKGGEKDPAKGVEKRPRVIQYP 165

                 Motif G                        Motif B
                                                      *
KFDV        403 KVRSNAALGA  412          601 QRGSGQVVTYALNTL 615
ALKV        403 KVRSNAALGA  412          601 QRGSGQVVTYALNTL 615
TBEV        403 KVKSNAALGA  412          601 QRGSGQVVTYALNTL 615
YEFV        403 KVRSHAAVGA  412          601 QRGSGQVVTYALNTI 615
ZKV         403 KVRSNAALGA  412          601 QRGSGQVVTYALNTF 615
JAEV        404 KVNSNAALGA  413          602 QRGSGQVVTYALNTF 616
WNV         404 KVNSNAALGA  413          602 QRGSGQVVTYALNTF 616
DEN_V2      401 KVRSNAALGA  411          599 QRGSGQVGTYGLNTF 613
HCV          90 LTPPHSAKSK  99           282 CRASGVLTTSCGNTL 296
```

*Fig. 5. Amino acid sequence alignment of motifs, F, G and B of NS5 from the flaviviridae family. Kyasanur forest disease virus (KFDV), Alkhurma hemorrhagic fever (ALKV), Tick borne encephalitis virus (TBEV), Yellow fever virus (YEFV), Zika virus (ZKV), Japanese encephalitis virus (JAEV), West Nile virus (WNV) Dengue virus serotype 2 (DENV2), Hepatitis C virus (HCV). Conserved residues in Motif F and motif G, from ring and pinky finger domains involved in interacting with NTPs and the template, respectively, are highlighted. Asn291 from NS5 RdRp domain of HCV makes a critical interaction with Sofosbuvir (42). Asn291 is highly conserved across the sequences shown in the figure (marked as *). There is a higher level of conservation among the genus, flavivirus as compared to flaviviruses and HCV (belongs to the genus Hepacivirus).*

As indicated earlier, active site residues in flaviviridae family are highly conserved, including Asn291 increasing the likelihood of Sofosbuvir inhibiting KFDV NS5. Sofosbuvir exhibited an IC_{50} of 6.83

µM against KFDV NS5 (Fig. 6). Interestingly, Dasabuvir, a non-nucleoside analogue, did not show inhibition of RdRp activity, even at 100 µM, under the tested conditions. IC_{50} of Dasabuvir varied between nM and µM against different genotypes of HCV RdRps (28). Also, Dasabuvir is not predicted to bind to conserved residues in RdRps across different viruses (43).

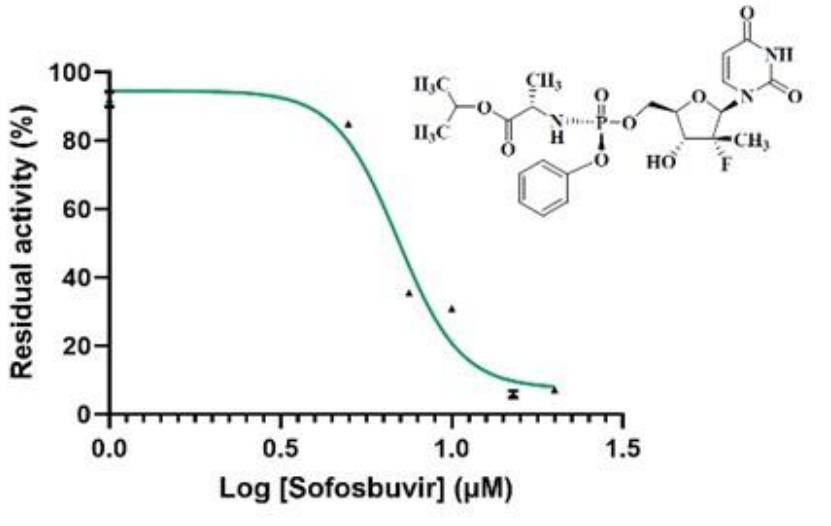

Fig. 6. Determination of IC_{50} for sofosbuvir. Increasing concentrations of Sofosbuvir was titrated using the optimized assay conditions as described in methods. Log of compound concentration is plotted against percentage activity and IC_{50}, computed from the profiles using Graph pad prism 9.3.0

Discussion

Kyasanur forest disease virus is a high-risk category pathogen, endemic to southern India. The current line of treatment for KFD include maintaining hydration, blood work, management of neurological and haemorrhagic conditions (6,11). Sofosbuvir, also known as L-Alanine,N-[[P(S),2'R]-2'-deoxy-2'-fluoro-2'-methyl-P-phenyl-5'-uridylyl]-,1-methyl ethyl ester ($C_{22}H_{29}FN_3O_9P$), is an orally available

nucleotide analogue, approved for the treatment of Hepatitis C viral infections (29). In preclinical studies, Sofosbuvir has been demonstrated to exhibit inhibitory activity against all genotypes of HCV (44). Sofosbuvir has been indicated for chronic HCV infection (genotype 1, 2, 3 or 4) in adults as part of combination therapy and in children, older than 3 years with genotype for chronic HCV infections with ribavirin. Many Clinical trials are ongoing for evaluating sofosbuvir in different populations and dosing regimens, in combination with other drugs against HCV (45 – 49). Sofosbuvir also exhibited inhibitory activity against Dengue, Chikungunya, Yellow fever virus, Hepatitis E virus and SARS-CoV2 (50 -54). KFDV NS5 expression construct, used in this study also included MTase domain, as methyl transferase domain was demonstrated to influence the activity RdRp domain by interaction with the template RNA (55). KFDV NS5 protein was recombinantly expressed in bacteria, and so were NS5 proteins from Usutu, Zika, Japanese encephalitis, Dengue, HCV and West Nile virus (34, 37, 40, 41, 55, 56). The Inhibitory concentration (IC_{50}) of sofosbuvir was found to be 6.84 µM with KFDV NS5. Consistent to this observation, recombinantly purified NS5 protein from Dengue Serotype 2, virus, exhibited an IC_{50} of 7.3 µM, and 14.7 µM, respectively, against sofosbuvir triphosphate and Sofosbuvir, respectively (57, 58). This is the first report of the expression and purification of NS5 protein of KFDV, its assay establishment and demonstration of inhibition of RdRp activity by sofosbuvir. Further, potential inhibitors of KFDV RdRp can be screened utilizing the established biochemical assay. Drug repurposing approaches against KFD, a neglected disease, can pave way for the

identification of novel inhibitors for the development of targeted therapeutic interventions against the disease.

References

1. Work TH, Trapido H, Murthy DP, Rao RL, Bhatt PN, Kulkarni KG. Kyasanur forest disease. III. A preliminary report on the nature of the infection and clinical manifestations in human beings. Indian J Med Sci. 1957;11(8):619-645.
2. Shah KV, Dandawate CN, Bhatt PN. Kyasanur forest disease virus: viremia and challenge studies in monkeys with evidence of cross-protection by Langat virus infection. F1000Res. 2012;1:61. doi:10.12688/f1000research.1-61.v1.
3. Muraleedharan K. Wildlife Arthropods of Karnataka with Special Reference to KFD Endemic Area of Shivamogga District: Those Parasitic on Small and Large Mammals. Veterinary Research International. 2016; 4(4): 114-123.
4. Varma MG, Webb HE, Pavri KM. Studies on the transmission of Kyasanur Forest disease virus by Haemaphysalis spinigera Newman. Trans R Soc Trop Med Hyg. 1960;54:509-516. doi:10.1016/0035-9203(60)90024-9.
5. Munivenkatappa A, Sahay RR, Yadav PD, Viswanathan R, Mourya DT. Clinical & epidemiological significance of Kyasanur forest disease. Indian J Med Res. 2018;148(2):145-150. doi:10.4103/ijmr.IJMR_688_17.
6. Shah SZ, Jabbar B, Ahmed N, Rehman A, Nasir H, Nadeem S, et al. Epidemiology, Pathogenesis, and Control of a Tick-Borne Disease-Kyasanur Forest Disease: Current Status and Future Directions.

Front Cell Infect Microbiol. 2018;8:149. doi:10.3389/fcimb.2018.00149.

7. Gupta N, Varma M, Saravu K. Difference in clinical presentation between the first and second phases of Kyasanur Forest disease: an experience from a teaching hospital in South India. Infez Med. 2020;28(4):597-602.
8. Majumdar T, Shete A, Yadav P, Patil S, Mali D, Waghmare A, et al. Point of care real-time polymerase chain reaction-based diagnostic for Kyasanur forest disease. Int J Infect Dis. 2021;108:226–30. doi:10.1016/j.ijid.2021.05.036.
9. Mourya DT, Yadav PD, Mehla R, et al. Diagnosis of Kyasanur forest disease by nested RT-PCR, real-time RT-PCR and IgM capture ELISA. J Virol Methods. 2012;186(1-2):49-54. doi:10.1016/j.jviromet.2012.07.019.
10. Kasabi GS, Murhekar MV, Sandhya VK, et al. Coverage and effectiveness of Kyasanur forest disease (KFD) vaccine in Karnataka, South India, 2005-10. PLoS Negl Trop Dis. 2013;7(1):e2025. doi:10.1371/journal.pntd.0002025.
11. Centers for Disease Control and Prevention. Fact Sheet: Kyasanur forest disease (KFD) [accessed on March 30, 2017]. https://www.cdc.gov/vhf/kyasanur/pdf/factsheet.pdf.
12. Dodd KA, Bird BH, Khristova ML, et al. Ancient ancestry of KFDV and AHFV revealed by complete genome analyses of viruses isolated from ticks and mammalian hosts. PLoS Negl Trop Dis. 2011;5(10):e1352. doi:10.1371/journal.pntd.0001352.
13. Bhatia B, Feldmann H, Marzi A. Kyasanur Forest Disease and Alkhurma Hemorrhagic Fever Virus-Two Neglected Zoonotic

Pathogens. Microorganisms. 2020;8(9):1406. doi:10.3390/microorganisms8091406.

14. Lin D, Li L, Dick D, et al. Analysis of the complete genome of the tick-borne flavivirus Omsk hemorrhagic fever virus. Virology. 2003;313(1):81-90. doi:10.1016/s0042-6822(03)00246-0

15. Wang J, Zhang H, Fu S, et al. Isolation of kyasanur forest disease virus from febrile patient, yunnan, china. Emerg Infect Dis. 2009;15(2):326-328. doi:10.3201/eid1502.080979.

16. Venugopal K, Gritsun T, Lashkevich VA, Gould EA. Analysis of the structural protein gene sequence shows Kyasanur Forest disease virus as a distinct member in the tick-borne encephalitis virus serocomplex. J Gen Virol. 1994;75(Pt1):227-232. doi:10.1099/0022-1317-75-1-227.

17. Wu J, Liu W, Gong P. A Structural Overview of RNA-Dependent RNA Polymerases from the Flaviviridae Family. Int J Mol Sci. 2015;16(6):12943-12957. doi:10.3390/ijms160612943.

18. Dong H, Fink K, Züst R, Lim SP, Qin CF, Shi PY. Flavivirus RNA methylation. J Gen Virol. 2014;95(Pt 4):763-778. doi:10.1099/vir.0.062208-0.

19. Elena SF, Sanjuán R. Adaptive value of high mutation rates of RNA viruses: separating causes from consequences. J Virol. 2005;79(18):11555-11558. doi:10.1128/JVI.79.18.11555-11558.2005.

20. Fernandes PO, Chagas MA, Rocha WR, Moraes AH. Non-structural protein 5 (NS5) as a target for antiviral development against established and emergent flaviviruses. Curr Opin Virol. 2021;50:30-39. doi:10.1016/j.coviro.2021.07.001.

21. Yao X, Guo S, Wu W, et al. Q63, a novel DENV2 RdRp non-nucleoside inhibitor, inhibited DENV2 replication and infection. J Pharmacol Sci. 2018;138(4):247-256. doi:10.1016/j.jphs.2018.06.012.

22. Arora R, Liew CW, Soh TS, et al. Two RNA Tunnel Inhibitors Bind in Highly Conserved Sites in Dengue Virus NS5 Polymerase: Structural and Functional Studies. J Virol. 2020;94(24):e01130-20. doi:10.1128/JVI.01130-20.

23. Chen Y, Li Z, Pan P, et al. Cinnamic acid inhibits Zika virus by inhibiting RdRp activity. Antiviral Res. 2021;192:105117. doi:10.1016/j.antiviral.2021.105117.

24. Lin Y, Zhang H, Song W, Si S, Han Y, Jiang J. Identification and characterization of Zika virus NS5 RNA-dependent RNA polymerase inhibitors. Int J Antimicrob Agents. 2019;54(4):502-506. doi:10.1016/j.ijantimicag.2019.07.010.

25. Coulerie P, Nour M, Maciuk A, et al. Structure-activity relationship study of biflavonoids on the Dengue virus polymerase DENV-NS5 RdRp. Planta Med. 2013;79(14):1313-1318. doi:10.1055/s-0033-1350672.

26. Abu-Zaied MA, Hammad SF, Halaweish FT, Elgemeie GH. Sofosbuvir Thio-analogues: Synthesis and Antiviral Evaluation of the First Novel Pyridine- and Pyrimidine-Based Thioglycoside Phosphoramidates. ACS Omega. 2020;5(24):14645-14655. doi:10.1021/acsomega.0c01364.

27. Sofia MJ, Bao D, Chang W, et al. Discovery of a β-d-2'-deoxy-2'-α-fluoro-2'-β-C-methyluridine nucleotide prodrug (PSI-7977) for the treatment of hepatitis C virus. J Med Chem. 2010;53(19):7202-7218. doi:10.1021/jm100863x.

28. Kati W, Koev G, Irvin M, et al. In vitro activity and resistance profile of dasabuvir, a nonnucleoside hepatitis C virus polymerase inhibitor. Antimicrob Agents Chemother. 2015;59(3):1505-1511. doi:10.1128/AAC.04619-14.

29. Gentile I, Borgia F, Buonomo AR, Castaldo G, Borgia G. A novel promising therapeutic option against hepatitis C virus: an oral nucleotide NS5B polymerase inhibitor sofosbuvir. Curr Med Chem. 2013;20(30):3733-3742. doi:10.2174/09298673113209990178.

30. Lawitz E, Jacobson IM, Nelson DR, et al. Development of sofosbuvir for the treatment of hepatitis C virus infection. Ann N Y Acad Sci. 2015;1358:56-67. doi:10.1111/nyas.12832.

31. Alves RPDS, Pereira LR, Fabris DLN, Salvador FS, Santos RA, Zanotto PM de A, et al. Production of a Recombinant Dengue Virus 2 NS5 Protein and Potential Use as a Vaccine Antigen. Clin Vaccine Immunol CVI. 2016;23(6):460–9. DOI: 10.1128/CVI.00081-16.

32. Del Campo J, Bouley J, Chevandier M, et al. OVX836 Heptameric Nucleoprotein Vaccine Generates Lung Tissue-Resident Memory CD8+ T-Cells for Cross-Protection Against Influenza. Front Immunol. 2021;12:678483. doi:10.3389/fimmu.2021.678483.

33. Sáez-Álvarez Y, Arias A, del Águila C, Agudo R. Development of a fluorescence-based method for the rapid determination of Zika virus polymerase activity and the screening of antiviral drugs. Sci Rep. 2019;9:5397.

34. Albentosa-González L, Clemente-Casares P, Sabariegos R, Mas A. Polymerase Activity, Protein-Protein Interaction, and Cellular Localization of the Usutu Virus NS5 Protein. Antimicrob Agents Chemother.;64(1):e01573-19.

35. Zhao Y, Soh TS, Zheng J, et al. A crystal structure of the Dengue virus NS5 protein reveals a novel inter-domain interface essential for protein flexibility and virus replication. PLoS Pathog. 2015;11(3):e1004682. doi:10.1371/journal.ppat.1004682.

36. Lim SP, Koh JHK, Seh CC, Liew CW, Davidson AD, Chua LS, et al. A crystal structure of the dengue virus non-structural protein 5 (NS5) polymerase delineates interdomain amino acid residues that enhance its thermostability and de novo initiation activities. J Biol Chem. 2013;288(43):31105–14. doi:10.1074/jbc.M113.508606.

37. Zhao B, Yi G, Du F, Chuang YC, Vaughan RC, Sankaran B, et al. Structure and function of the Zika virus full-length NS5 protein. Nat Commun. 2017;8(1):14762. doi:10.1038/ncomms14762.

38. Lohmann V, Roos A, Körner F, Koch JO, Bartenschlager R. Biochemical and kinetic analyses of NS5B RNA-dependent RNA polymerase of the hepatitis C virus. Virology. 1998;249(1):108-118. doi:10.1006/viro.1998.9311.

39. Saisawang C, Kuadkitkan A, Auewarakul P, Smith DR, Ketterman AJ. Glutathionylation of dengue and Zika NS5 proteins affects guanylyltransferase and RNA dependent RNA polymerase activities. PLoS One. 2018;13(2):e0193133. doi: 10.1371/journal.pone.0193133.

40. Lu G, Gong P. Crystal Structure of the full-length Japanese encephalitis virus NS5 reveals a conserved methyltransferase-polymerase interface. PLoS Pathog. 2013;9(8):e1003549. doi:10.1371/journal.ppat.1003549.

41. Potisopon S, Priet S, Collet A, Decroly E, Canard B, Selisko B. The methyltransferase domain of dengue virus protein

NS5 ensures efficient RNA synthesis initiation and elongation by the polymerase domain. Nucleic Acids Res. 2016;44(6):2974. doi:10.1093/nar/gkv1294.

42. Appleby TC, Perry JK, Murakami E, Barauskas O, Feng J, Cho A, et al. Structural basis for RNA replication by the hepatitis C virus polymerase. Science. 2015;347(6223):771–5. doi:10.1126/science.1259210.

43. de Albuquerque PPLF, Santos LHS, Antunes D, Caffarena ER, Figueiredo AS. Structural insights into NS5B protein of novel equine hepaciviruses and pegiviruses complexed with polymerase inhibitors. Virus Res. 2020;278:197867. doi:10.1016/j.virusres.2020.197867.

44. Han B, Martin R, Xu S, et al. Sofosbuvir susceptibility of genotype 1 to 6 HCV from DAA-naïve subjects. Antiviral Res. 2019;170:104574. doi:10.1016/j.antiviral.2019.104574.

45. Chua J. A Phase II Open-Label Study of Ledipasvir/Sofosbuvir for 12 Weeks in Subjects with Hepatitis B Virus Infection [Internet]. clinicaltrials.gov; 2021 Aug [cited 2022 Jun 15]. Report No.: NCT03312023. Available from: https://clinicaltrials.gov/ct2/show/NCT03312023.

46. Hospices Civils de Lyon. Sofosbuvir Plus Daclatasvir With or Without Ribavirin for Chronic Hepatitis C Infection: Impact of Drug Concentration on Viral Load Decay [Internet]. clinicaltrials.gov; 2017 Oct [cited 2022 Jun 15]. Report No.: NCT03318887. Available from: https://clinicaltrials.gov/ct2/show/NCT03318887.

47. El-Sayed MH. Clinical Pharmacokinetics, Safety and Efficacy Study of Daclatasvir/Sofosbuvir in Adolescents Aged 12

to 18 Years Old With Hepatitis C Virus: A Preliminary Study [Internet]. clinicaltrials.gov; 2019 Mar [cited 2022 Jun 15]. Report No.: NCT03540212. Available from: https://clinicaltrials.gov/ct2/show/NCT03540212.

48. Elmoety AAA. Evaluation of Sofosbuvir and Daclatasvir Combo in COIVD-19 Patients in Egypt (Single Center Study) [Internet]. clinicaltrials.gov; 2021 Feb [cited 2022 Jun 15]. Report No.: NCT04773756. Available from: https://clinicaltrials.gov/ct2/show/NCT04773756.

49. Chappell C. Safety, Tolerability, and Outcomes of Velpatasvir/SofosbuviR in Treatment of Chronic Hepatitis C Virus During Pregnancy (STORC) [Internet]. clinicaltrials.gov; 2022 Apr [cited 2022 Jun 15]. Report No.: NCT05140941. Available from: https://clinicaltrials.gov/ct2/show/NCT05140941.

50. Xu HT, Colby-Germinario SP, Hassounah SA, Fogarty C, Osman N, Palanisamy N, Han Y, Oliveira M, Quan Y, Wainberg MA. Evaluation of Sofosbuvir (β-D-2'-deoxy-2'-α-fluoro-2'-β-C-methyluridine) as an inhibitor of Dengue virus replication. Sci Rep. 2017 Jul 24;7(1):6345. doi: 10.1038/s41598-017-06612-2. PMID: 28740124; PMCID: PMC5524696.

51. Ferreira AC, Reis PA, de Freitas CS, et al. Beyond Members of the Flaviviridae Family, Sofosbuvir Also Inhibits Chikungunya Virus Replication. Antimicrob Agents Chemother. 2019;63(2):e01389-18. doi:10.1128/AAC.01389-18

52. de Freitas CS, Higa LM, Sacramento CQ, et al. Yellow fever virus is susceptible to sofosbuvir both in vitro and in vivo. PLoS Negl Trop Dis. 2019;13(1):e0007072. doi:10.1371/journal.pntd.0007072HEV-SF

53. Liang Z, Shu J, He Q, et al. High dose sofosbuvir and sofosbuvir-plus-ribavirin therapy inhibit Hepatitis E Virus (HEV) replication in a rabbit model for acute HEV infection. Antiviral Res. 2022;199:105274. doi:10.1016/j.antiviral.2022.105274

54. Sacramento CQ, Fintelman-Rodrigues N, Temerozo JR, et al. In vitro antiviral activity of the anti-HCV drugs daclatasvir and sofosbuvir against SARS-CoV-2, the aetiological agent of COVID-19. J Antimicrob Chemother. 2021;76(7):1874-1885. doi:10.1093/jac/dkab072

55. Rusanov T, Kent T, Saeed M, et al. Identification of a Small Interface between the Methyltransferase and RNA Polymerase of NS5 that is Essential for Zika Virus Replication. Sci Rep. 2018;8(1):17384. doi:10.1038/s41598-018-35511-3.

56. Oh JW, Ito T, Lai MM. A recombinant hepatitis C virus RNA-dependent RNA polymerase capable of copying the full-length viral RNA. J Virol. 1999;73(9):7694-702. doi: 10.1128/JVI.73.9.7694-7702.1999.

57. Nomaguchi M, Teramoto T, Yu L, Markoff L, Padmanabhan R. Requirements for West Nile Virus (-)- and (+)-Strand Subgenomic RNA Synthesis in Vitro by the Viral RNA-dependent RNA Polymerase Expressed in *Escherichia coli*. J Biol Chem. 2004;279:12141–51. doi:10.1074/jbc.M310839200.

58. Xu HT, Colby-Germinario SP, Hassounah SA, Fogarty C, Osman N, Palanisamy N, et al. Evaluation of Sofosbuvir (β-D-2′-deoxy-2′-α-fluoro-2′-β-C-methyluridine) as an inhibitor of Dengue virus replication. Sci Rep. 2017;7(1):6345. doi:10.1038/s41598-017-06612-2.

59. Xu HT, Hassounah SA, Colby-Germinario SP, Oliveira M, Fogarty C, Quan Y, Han Y, Golubkov O, Ibanescu I, Brenner B, Stranix BR, Wainberg MA. Purification of Zika virus RNA-dependent RNA polymerase and its use to identify small-molecule Zika inhibitors. J Antimicrob Chemother. 2017;72(3):727-734. doi: 10.1093/jac/dkw514.

Acknowledgements

The authors would like to thank Tata Institute for Genetics and Society for funding this study. We would like to acknowledge the NCBS-inStem-CCAMP mass spectrometry facility for technical assistance, provided for this study.

Conflict of interest

The authors declare no conflict of interests.

Availability of data and materials

All the relevant data used to support the findings of this study are included within the article.